International Journal of Environmental Sciences
ISSN: 2229-7359
Vol. 11 No. 21s, 2025
https://theaspd.com/index.php

Probabilistic Mapping And Sensitivity Assessment Of Dam Breach Flood Inundation

Neman Sharif M.M[1], Dr. Inayathulla M[2]
[1]Research Scholar, DCE, University of Visvesvaraya College of Engineering, Bengaluru
[2]Professor, DCE, University of Visvesvaraya College of Engineering, Bengaluru, Karnataka, India

Abstract *- Dam breach floods present severe threats to downstream populations, infrastructure, and ecosystems. This study conducts a probabilistic flood inundation mapping and sensitivity analysis for the Almatti Dam on the Krishna River, Karnataka, India. The latitude and longitude of the Almatti dam site are 16°19'00"N and 75°53'15" E respectively. The dam is a blend of earth-fill and masonry construction, stretching over 1,564.83 meters in length and height of 49.29 meters. It holds a substantial storage capacity of around 123 TMC and manages water from a vast catchment area of about 35,925 square kilometers. The project is jointly managed by two government agencies: Krishna Bhagya Jala Nigam Limited (KBJNL), responsible for water storage, reservoir operations, and irrigation management, and Karnataka Power Corporation Limited (KPCL), which operates the hydroelectric plant with an installed capacity of up to 290 MW. Using a Monte Carlo simulation framework integrated with HEC-RAS 2D hydrodynamic modeling, uncertainty in breach parameters (e.g., breach width, formation time) and hydrological inputs (e.g., inflow hydrographs, Manning's roughness) is incorporated to generate probabilistic flood hazard maps. Exceedance probabilities of inundation extents, depths, and arrival times are derived from multiple simulated scenarios. Sensitivity analysis identifies breach size, formation time, and reservoir level as the most influential factors in downstream hazard magnitude. The results provide a robust basis for flood risk assessment, supporting Almatti dam authorities in designing effective emergency action plans, evacuation strategies, and early warning systems by explicitly accounting for uncertainty in dam-break events.*

Key Words: *Flood Inundation Mapping, hydrologic, hydraulic modelling, Dam breach analysis, HEC-RAS · HEC-HMS. Dam breach, Probabilistic flood mapping, Monte Carlo simulation.*

1.INTRODUCTION :

Dams are essential infrastructure for water conservation and a nation's economy, serving multiple purposes like electricity generation, flood control, and irrigation. However, dam failures, while rare, can lead to catastrophic flooding, resulting in loss of life, property damage, and environmental changes. Earthen dams, being a common and cost-effective type, are particularly susceptible to failure due to their lower structural rigidity, with overtopping and piping being the most frequent causes.

Although a dam-break event is quite rare [1], the non-negligible number of historical dam disasters documented [[2], [3], [4]] indicates that this catastrophic event cannot be excluded. Dam-break inundation studies are essential for flood risk management, emergency response planning and preparedness, and development of flood mitigation measures to minimize loss of life and property damage [[5], [6], [7]].

Dam safety guidelines and technical regulations issued by various governments and national agencies mandate dam owners to conduct dam-break analyses for the preparation of Emergency Action Plans (EAPs) and to establish dam hazard potential classifications [[8]. [9]; [10]; [11]].

Earthen dams are widely recognized as one of the most prominent dam types due to their versatility in accommodating various foundation conditions, straightforward construction processes, and relatively economical cost [[12], [13]]. Nevertheless, clay dams, owing to their lower structural rigidity, exhibit an increased susceptibility to failure [14]. A dam breach is characterized as either a partial or a catastrophic failure, resulting in uncontrolled downstream flooding [[15], [16]]. When a dam breaches, it generates a flood wave of increased height and velocity, thereby exerting a significant impact on both downstream life and property [[17], [18]]. Despite the incorporation of sufficient safety margins in dam engineering, their failure can still occur due to various factors, such as leakage, overtopping, seepage, seismic events, and other natural disasters [[19], [20], [21]]. The necessity for dam break analysis arises from the inherent risk of dam failure and its far-reaching consequences. Such analyses play a crucial role in assisting decision-makers with land use planning and the formulation of emergency response strategies, ultimately aimed at mitigating the potentially catastrophic loss of life and property damage [[22] [23]].

While deterministic approaches are common in dam-break studies, they often overlook uncertainties in hydrological conditions, breach formation, and topography. **Probabilistic methods**, such as **Monte Carlo simulations**, offer a more robust framework by incorporating variability in key parameters to generate **flood hazard maps with confidence intervals**.

This study advances **probabilistic dam-break flood modeling**, emphasizing concrete/masonry dams, and assess how input uncertainties propagate into flood predictions.

2 STUDY AREA

The Almatti Reservoir, located on the Krishna River in Karnataka, India, has a catchment area of approximately 35,925 km². It forms part of the Upper Krishna Irrigation Project, receiving inflows primarily from Karnataka and Maharashtra. The location of the study area is as shown in Figure No.1

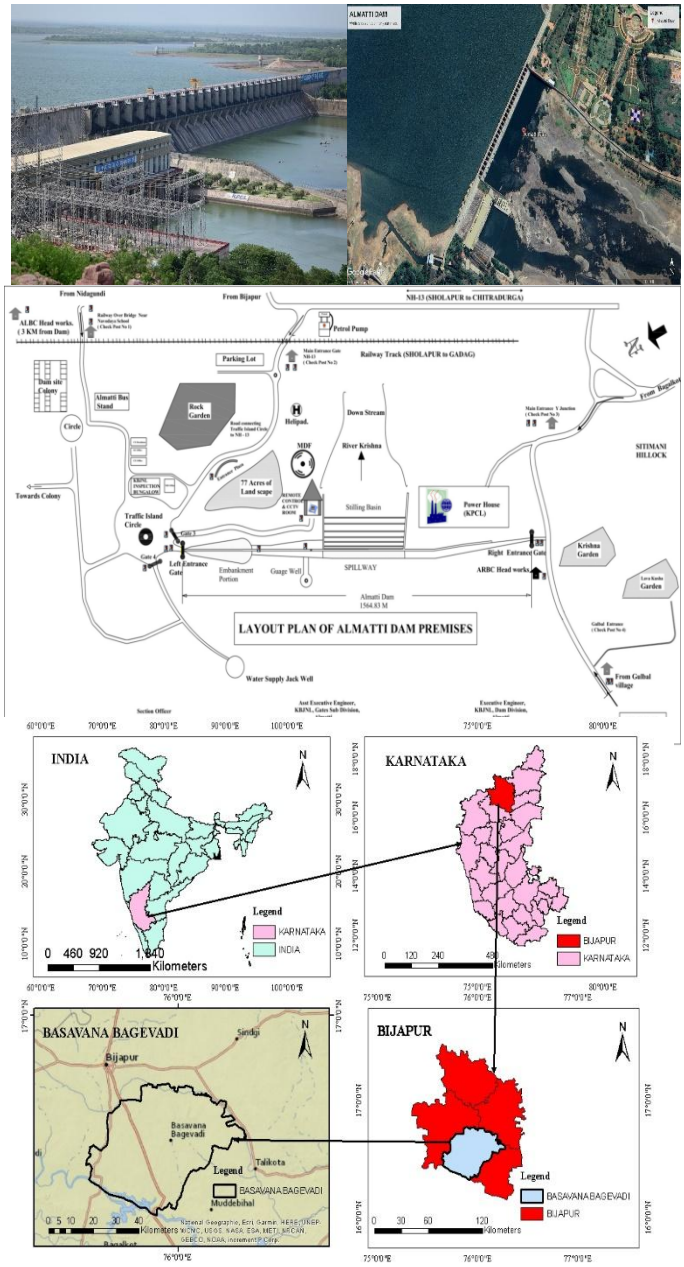

Figure No.1: Location map of the Study area

The Krishna River's flow is highly seasonal, driven by monsoon rainfall, with an average annual yield of about 116 TMC (thousand million cubic feet). The dam plays a key role in regulating this yield for irrigation, drinking water supply, and hydropower generation. It has a Full Reservoir Level (FRL) of 519.6 m, a gross storage capacity of 123.08 TMC (3,480 MCM), and a live storage capacity of 105.46 TMC (2,986.63 MCM), with the remaining 17.62 TMC (500 MCM) as dead storage. In addition to supplying water for agriculture and domestic use, the dam supports hydroelectric power generation with an installed capacity of 290 MW. The salient features of Almatti reservoir project is tabulated in Table No.1.

Table No.1: Salient features of Almatti Reservoir Project

Embankment	
Type	Masonry and Zoned Earth Fill
Length	402 m
Maximum Height	40.5 m
Top Width	9.00 m
Tope of Embankment Elevation	529.25 m MSL
Drainage Area	35.93 Square kilometres
Main Spillway	
Type	Gated Ogee
Crest Length	486.50 m
Crest Elevation	509.02 m
Capacity	47318 cumecs
Inlet Outlet Works	
Type	Regular Gates
Invert Elevation (Inlet)	517.00m MSL
Invert Elevation (Outlet)	517.00m MSL
Capacity	14.91 cumecs
Reservoir	
Elev. Top of Conservation Pool	519.60 m MSL
Capacity Normal Pool	2986.26 millions of cubic m
Capacity at Top of Dam	3485.21 millions of cubic m
Surface Area	48787 hectares
Catchment area	35,925 Sq km

Figure no. 2 illustrates the elevation-area relationship of the Almatti reservoir,

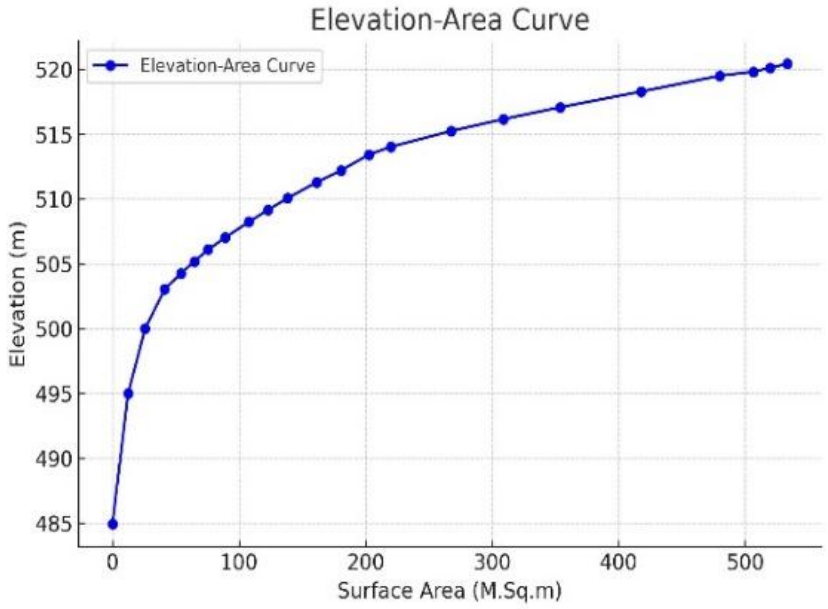

Figure No.2: Elevation Area curve.

Figure no. 3, 4 & 5 depicts the elevation storage curve, rule curve elevation and PMF Hydrograph.

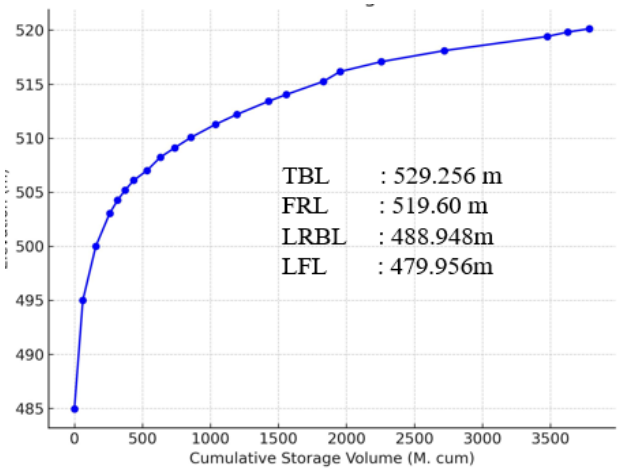

Figure No.3: Elevation-Storage curve

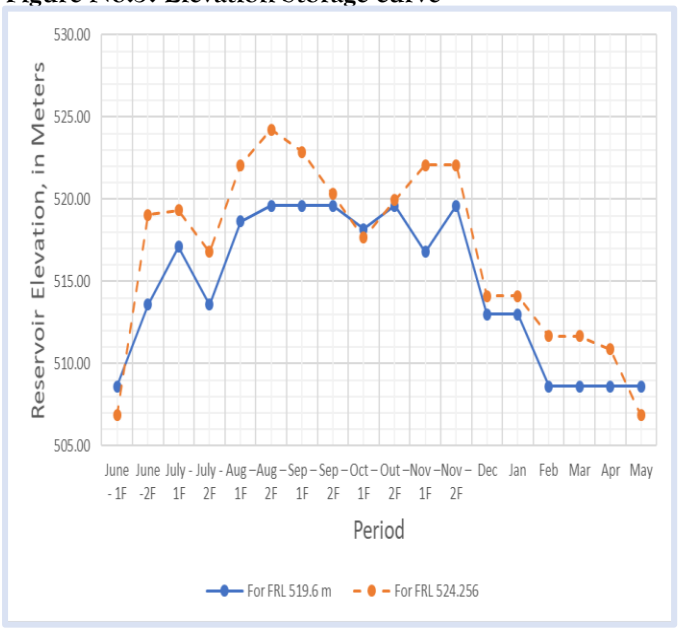

Figure No.4 – Almatti Dam Rule Curve Elevations

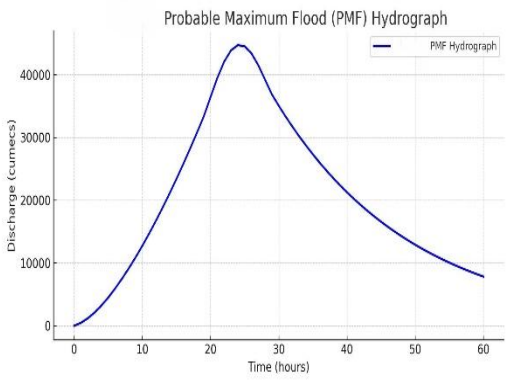

Figure No.5: PMF Hydrograph

Furthermore, numerous villages located downstream of the dam would be affected in the event of a dam-break–induced flood, as shown in Figure 6. Therefore, the inundation mapping developed in this study is particularly relevant and valuable in this context.

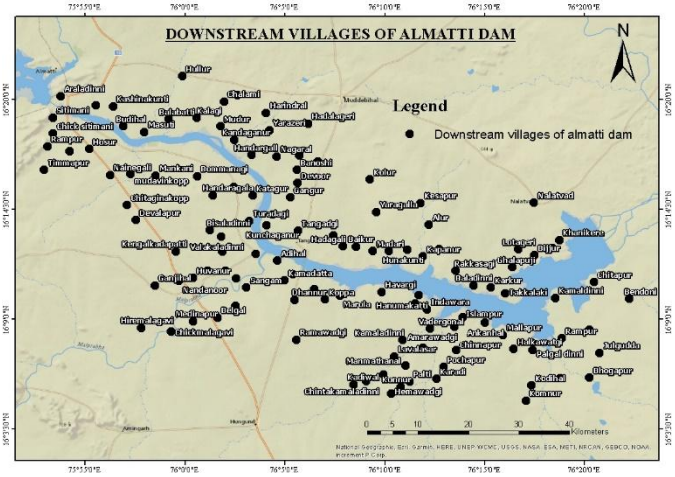

Figure No.6: Downstream Villages of Almatti Dam

3. Probabilistic flood hazard mapping

The probability $P_{i,j}$ associated with the (i,j) scenario is defined as the conditional probability that, given a dam-break event B the event will unfold according to scenario $S_{i,j}$ such that

$$P_{i,j} = P\left(S_{i,j}\middle|B\right) = P\left((H_{i+1} \le H \le H_f) \cap (L_{i+1} \le L \le L_f)\middle|B\right)$$

The joint probability rule for independent events is

$$P\left((H_{i+1} \le H \le H_f) \cap (L_{i+1} \le L \le L_f)\middle|B\right) = P\left((H_{i+1} \le H \le H_f)\middle|B\right).P\left((L_{i+1} \le L \le L_f)\middle|B\right)$$

The joint probability rule for dependent events is

$$P[(H_{i+1} \le H \le H_f) \cap B] = P\left((H_{i+1} \le H \le H_f)\middle|B\right).P(B)$$

$$P[(H_{i+1} \le H \le H_f) \cap B] = \int_{H_{i+1}}^{H_i} P(H)\,P(B|H)dH$$

$$P\left((H_{i+1} \le H \le H_f)\middle|B\right) = \frac{1}{P(B)}\int_{H_{i+1}}^{H_i} P(H)\,P(B|H)dH$$

4. Probabilistic inundation extent map

The probabilistic inundation extent map illustrates the spatial distribution of inundation probability in the event of a dam-break, thereby inherently conveying the uncertainty associated with flood extent [[24], [25]]. This map is derived by combining the inundation probability outputs from all simulated dam-break scenarios.

$$A_{i,j}(x,y) = \begin{cases} 0 & \text{if } HR_{i,j}(x,y) = 0 \\ P_{i,j} & \text{if } HR_{i,j}(x,y) > 0 \end{cases}$$

The probabilistic inundation extent map is then obtained by

$$P_{in}(x,y) = \sum_{i=0}^{N_H-1}\sum_{j=0}^{N_L-1} A_{i,j}(x,y)$$

with Pin being the inundation probability

5. Probabilistic flood hazard maps

The probability that, in the event of a dam-break, the k^{th} hazard class (k=0,1,..., 4) will occur at location (x,y) is defined as

$$P_{HC=k}(x,y) = \sum_{i=0}^{N_H-1}\sum_{j=0}^{N_L-1} C_{(i,j|HC=k)}(x,y)$$

The uncertainty in the local "expected" flood hazard can be expressed as

$$rCV(x,y) = \frac{\sigma_{HR}(x,y)}{\mu_{HR}(x,y)}\,\frac{1}{\sqrt{N_H N_L - 1}}$$

Standard deviation is given by

$$\sigma_{HR}(x,y) = \sqrt{\sum_{i=0}^{N_H-1}\sum_{j=0}^{N_L-1} P_{i,j}[HR_{i,j}(x,y) - \mu_{HR}(x,y)]^2}$$

6. FLOOD INUNDATION MAPPING

The mapping of inundated area will be made using HEC-Geo-RAS, which is an ArcGIS based pre- and post-processor for HEC-RAS. The methodology adopted is shown in Figure no.5.

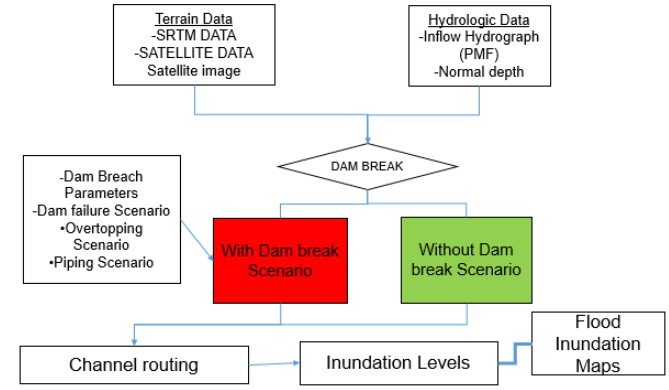

Figure No.5: Flow Chart for Methodology of 2-D Modeling using HEC-RAS

The major interventions in the study area, along with the land use and land cover map and the status indication map, are presented in Plate no. 1, Figure no.6 , and Plate no.3.

Plate No.1: Major Intervention locations

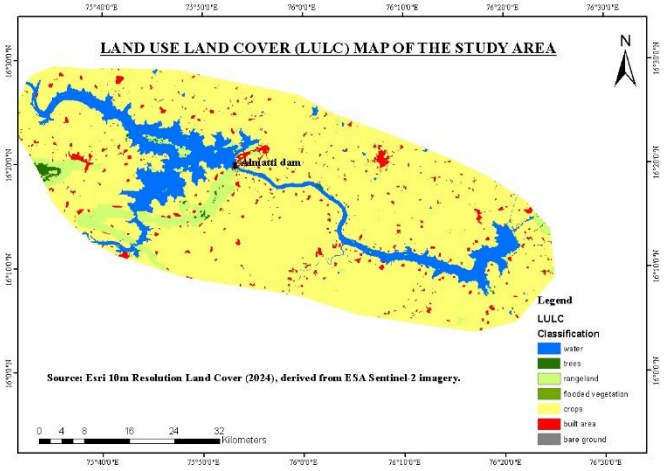

Figure No.6: Land use Land Cover (LULC) Map

Plate no.2: Status Indication map of Almatti Dam
Item: 1. Status indication for the PLC. It becomes Green when the PLC (or Gate) is on.
Item: 2. The UI Switch to take the user to the Respective Station
Item: 3. The UI Button to take the user to over View screen
Item: 4. The UI Button to popup the login Screen. unless the User Logs-in, the user will not be able to go to 'Overview' Screen or perform any Gate Lifting Operations.
Item: 5. The Reservoir Level Indication.

7. Hydrodynamic Model Setup

The terrain data of the study area (Plate no.1) was processed to generate a computational mesh for the 2D hydrodynamic model [[26], [27]]. The outer boundary of the mesh was delineated using a polygon, with computational cells along the boundary defined by multipoint lines representing their outer faces. The 2D flow area was hydraulically connected to the upstream storage area through an inline structure representing the dam.

Boundary conditions were assigned following established procedures [[28]. [29]]. An upstream flow hydrograph, is applied as the inlet condition, with data entered into the 2D unsteady flow editor [30]. For the downstream boundary, a normal depth condition was specified, consistent with the 1D modeling approach [31].

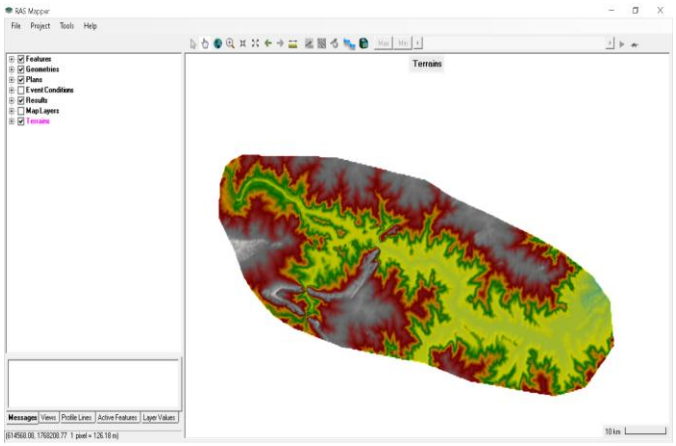

Plate no. 1: Creation of Terrain profile in HEC-RAS using RAS mapper

Model simulations (Fig. no.7) generated spatially distributed outputs, including flood depth, velocity, flow area, and maximum water surface elevation.

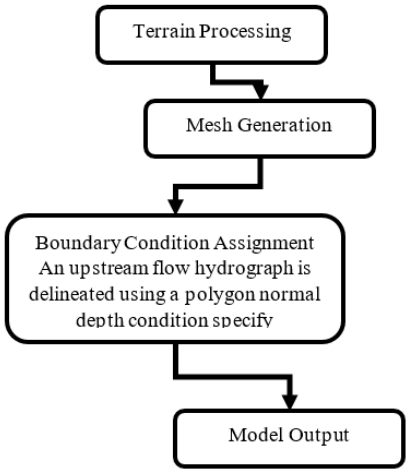

Figure no.7: schematic or workflow diagram

The estimation of the breach location, size and development time are to be done in order to make an accurate estimate of downstream inundation. The HEC-RAS software requires the user to enter the following information to describe a dam breach.

- **Failure location:**
- **Failure mode:** Overtopping or piping.
- **Time:** Critical breach development time
- **Breach weir and piping flow coefficients:**
- **Breach Shape:** Bottom elevation, bottom width, left and Right side slopes H: V.

A diagram describing the breach presented in Figure no. 8

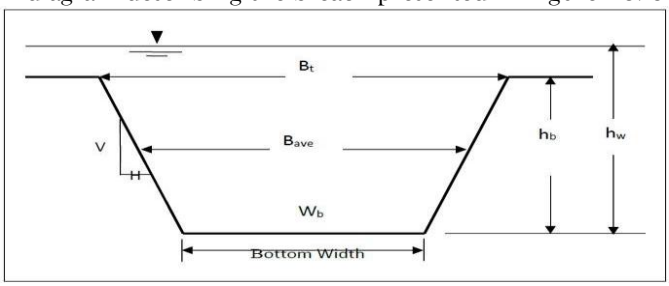

Figure no.8: Description of the Breach Shape

where,

B_{ave} = Average breach width.

W_b = Breach bottom width.

B_t = Breach top width.

h_b = Height of breach in m

h_w = Height of the water, which is the vertical extent from the maximum water surface to the invert elevation of the breach.

H: 1V = Side slopes expressed in units of distance horizontal to every one unit in vertical.

Breach Parameter Estimates is tabulated in Table no.2 and unsteady flow data, 2D mesh storage area are presented in Plates no. 3 to 5.

Table No.2: Trapezoidal Dam Breach model Parameter

Breach parameter	Units	Dam Failure Mode	
		Overtopping	Internal erosion (piping)
Height	m	40.3	40.3
Bottom width	m	560	480
Average side slope (horz : vert)	--	vertical	vertical
Formation time	h	0.25	0.25
Calculated peak discharge	m^3/s	123,427	85,834

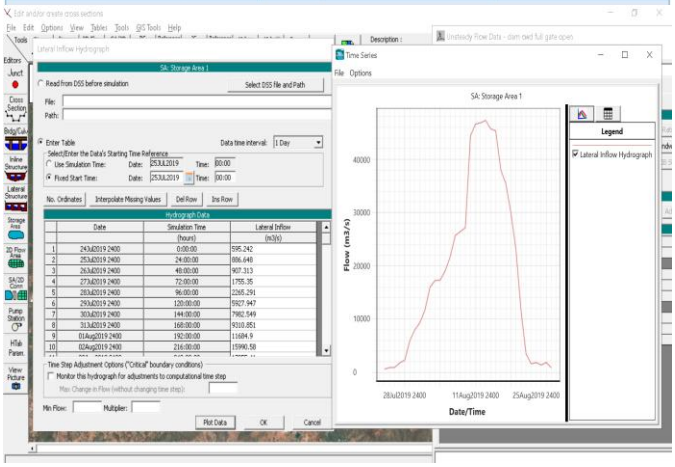

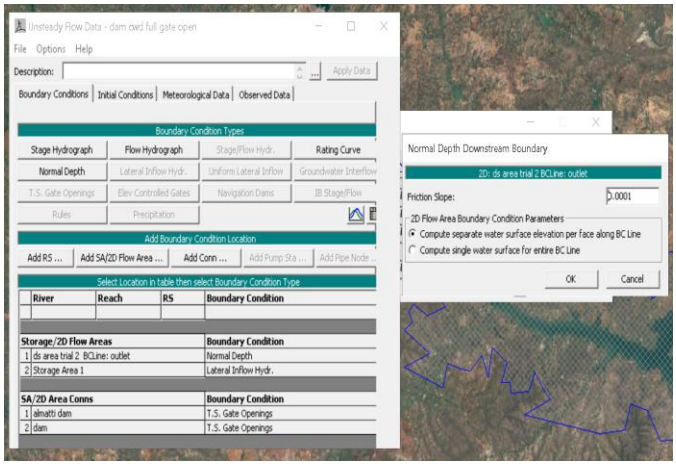

Plate No.3: Unsteady Flow Data for 2-D Modeling

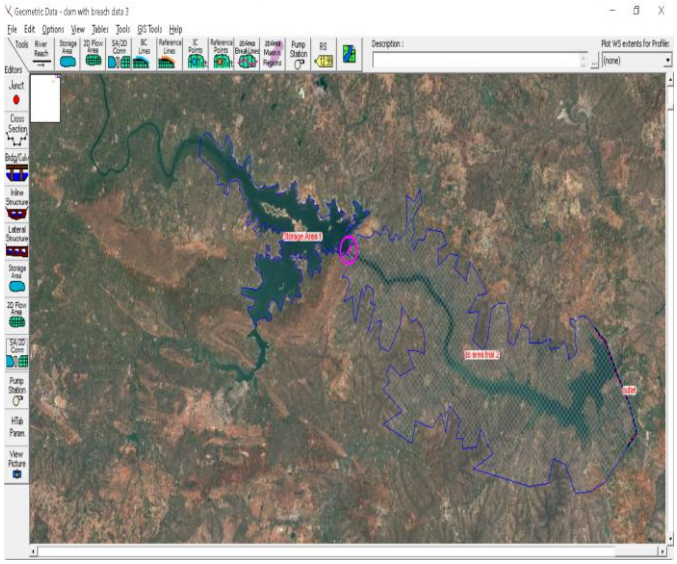

Plate No.4: shows the storage area and 2D flow Mesh of the study area

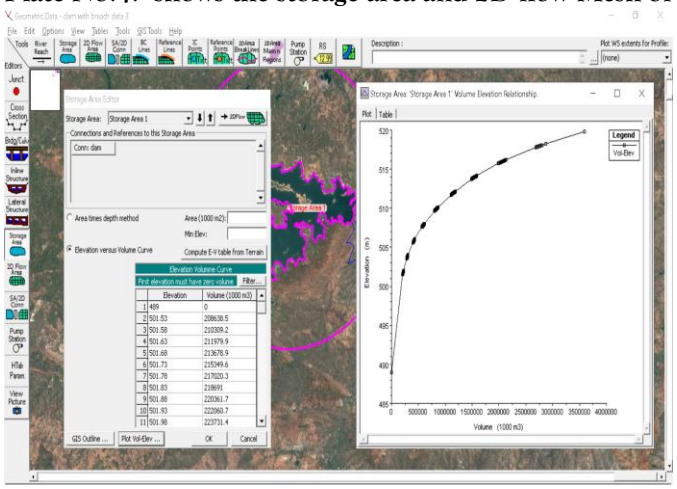

Plate no.5: shows the Storage elevation relationship of the Study area

8. RESULTS AND DISCUSSIONS

The model has been run assuming that the lateral flows impinge on various chainages. Two Full Reservoir Level (FRL) conditions that is EL 519.60m and EL524.25m has been considered and it is assumed that the maximum probable flood (PMF) of 31007 impinges when the reservoir is at FRL Manning's Roughness coefficient n value has been assumed based on the bed conditions and topography of the area. Plots of the backwater profiles for the following three scenarios are given below:

- PMF of 317007 cumec under natural flow conditions considering Manning's n value of 0.028.
- PMF of 317007 cumec impinging at FRL of 519.60m considering Manning's n value of 0.028.
- PMF of 317007 cumec impinging at FRL of 524.25m considering Manning's n value of 0.028.

The study utilized a **2D HEC-RAS model** to generate flood inundation maps for a dam breach scenario, considering different failure modes and breach parameters derived from various regression equations. The results are presented in two main categories:

1) **Flood Inundation Maps with a Dam-Break Scenario :** These maps were created by simulating a dam breach using breach parameters calculated from different regression equations. The simulations were conducted for two distinct failure modes:

- **Overtopping Failure:** The model simulated a dam breach caused by water flowing over the top of the dam. The resulting **2D flood inundation maps** depict the extent, depth, and velocity of the floodwaters in the downstream area.
- **Piping Failure:** The model simulated a breach initiated by internal erosion, or "piping," within the dam structure. These **2D flood inundation maps** illustrate the flood's characteristics, providing a visual representation of how this type of failure would impact the downstream region.

From Figure no. 9 to **Error! Reference source not found.** there shows various villages which are inundated.

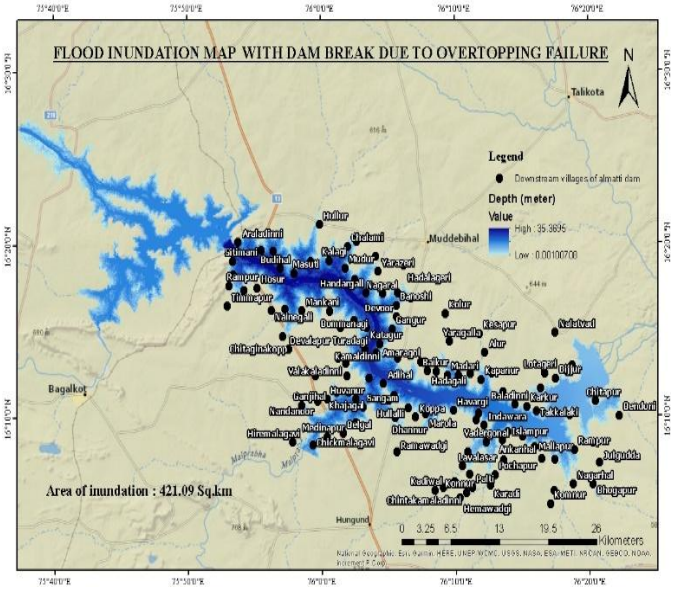

Figure no. 9 Flood Inundation Mapping with Dam Break due to Overtopping Failure.

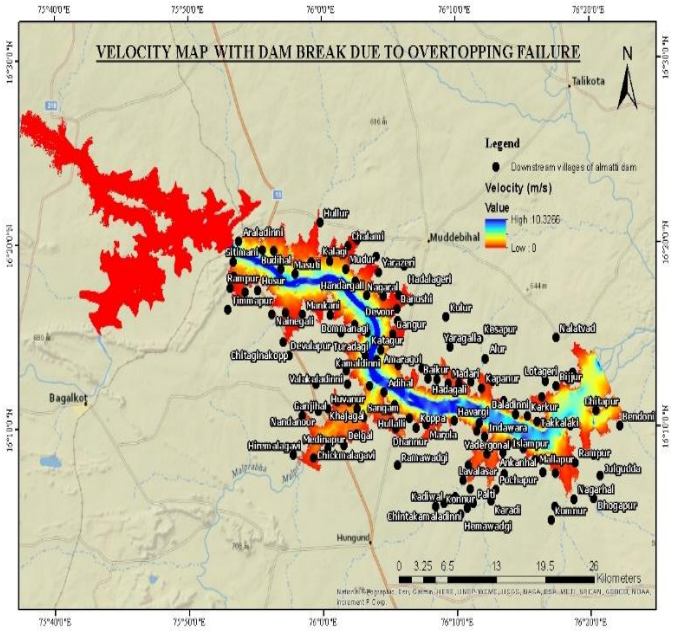

Figure no.10: Velocity with Overtopping Failure

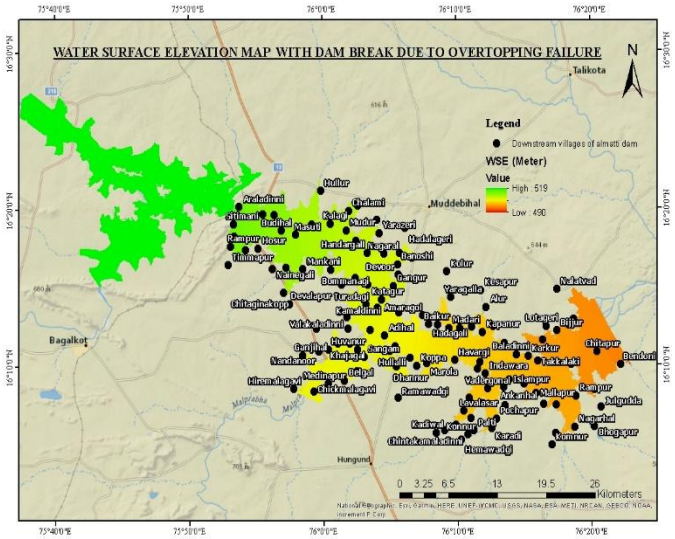

Figure no.11: Water surface elevation with Dam Break analysis due to Overtopping Failure

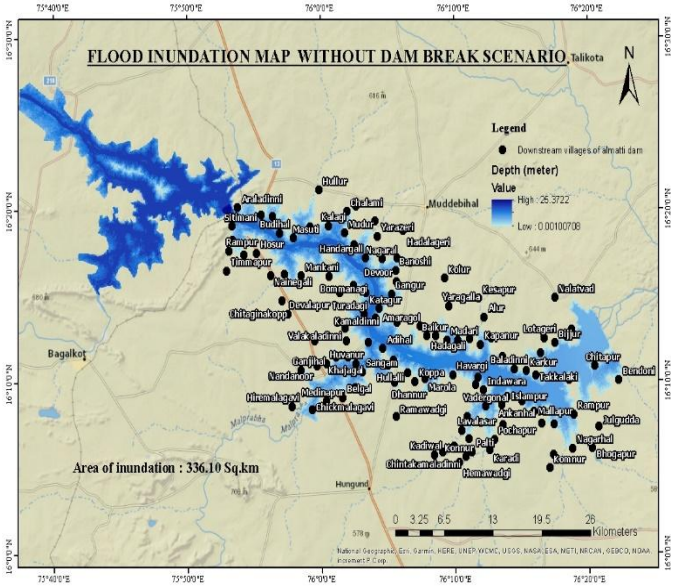

Figure no. 12: Flood Inundation Map without Dam Break Scenario

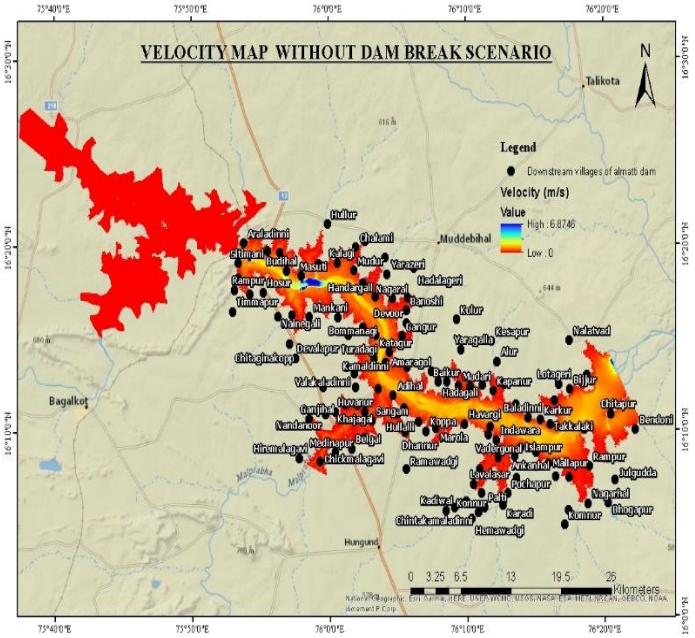

Figure no. 13: Velocity without Dam Break Scenario

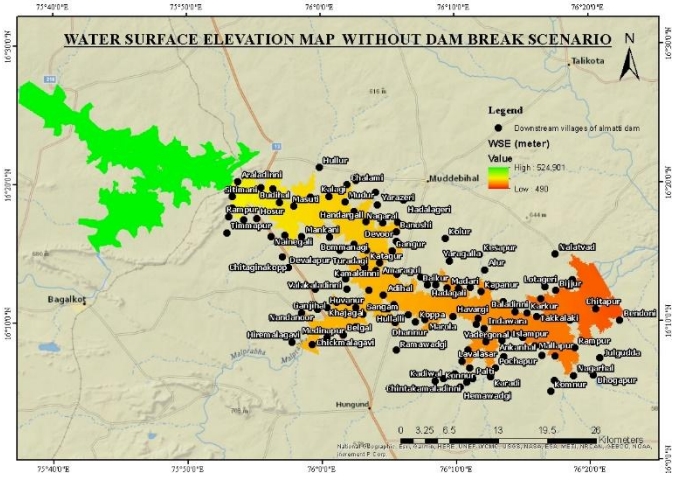

Figure no. 14: Water Surface Elevation map without Dam Break Scenario

9. CONCLUSIONS

The study's methodology is grounded in the understanding that masonry dams like Almatti fail rapidly, justifying the assumption of an **instantaneous breach**. This assumption, along with the use of Froehlich's empirical methods for estimating breach parameters, aligns with established guidelines and literature from the Central Water Commission (CWC). This approach ensures that the dam-break model is based on realistic and accepted engineering practices for sudden failures.

A dam-break scenario, specifically an overtopping failure, would result in a highly destructive flood wave. The simulated maximum flood wave velocity is **11.28 m/s**, which is extremely high and poses a severe threat to downstream life and property. The flood's impact is also characterized by significant changes in water surface elevation, ranging from a minimum of **614.166 m** to a maximum of **755.139 m**. This vast difference indicates a powerful and destructive surge of water.

Comparing the "without dam-break" scenario (PMF analysis) to the "with dam-break" scenario reveals a drastic increase in the scale of flooding. The PMF analysis showed a maximum inundation area of **421.09 Sq. km**, which represents the baseline flood risk. A dam breach would significantly exceed this. Additionally, the study highlights a crucial finding: **urban areas are more susceptible to variations in flood inundation** than non-urban areas. This is likely due to the higher concentration of impervious surfaces in cities, which can alter flood discharge rates and amplify the flood's impact

8 PRACTICAL IMPLICATIONS:

These findings highlight the necessity for robust Emergency Action Plans (EAPs) that consider instantaneous breach scenarios and account for uncertainty in flood propagation. The velocity and elevation data provide critical input for evacuation planning, structural resilience measures, and prioritization of downstream protection works. The greater vulnerability of urban areas underscores the need for targeted interventions, such as improved stormwater management and rapid alert systems, to reduce loss of life and property damage in the event of an Almatti Dam failure.

REFERENCES

[1] Hinks, J.L., Kitamura, Y., and Murphy, A.T., "Risk analyses for large dams.," in 13th ICOLD International Benchmark Workshop on the Numerical Analysis of Dams, , 9–11 September 2015, Lausanne, Switzerland. Swiss Committee on Dams, 277–284. Available from: https://www.itcold.it/wpsysfiles /wp-content/uploads/2018/02/ ICOLD _ Compudams _ BW13_Lausanne_2015.pdf [Accessed 28 Oct 2022]. , 2015.

[2] International Commission on Large Dams, "Dam failures. Statistical analysis," in (Bulletin 99). Paris, France: ICOLD., 1995.

[3] Zhang, L., et al., , "Dam failure mechanisms and risk assessment.," in Singapore: Wiley. , 2016.

[4] Aureli, F., Maranzoni, A., and Petaccia, G.,, "Review of historical dam-break events and laboratory tests on real topography for the validation of numerical models.," Water, 8 , vol. doi:10.3390/ w1314196, pp. 13 (14), 1968. , 2021.

[5] Rodrigues, A.S., et al.,, "Dam-break flood emergency management system.," Water Resources Management, , Vols. 16 (6),doi:10.1023/ A:1022225108547, p. 489–503. , 2002.

[6] Viseu, T. and Betâmio de Almeida, A.,, "Dam-break risk management and hazard mitigation.," in In: WIT Transactions on State-of-the-art in Science and Engineering. Southampton, UK, WIT Press, 36, 211– 239. doi:10.2495/978-1-84564-142-9/06, 2009.

[7] Albano, R., et al.,, "A GIS tool for mapping dam-break flood hazards in Italy," ISPRS International Journal of Geo-Information,, Vols. 8 (6), , p. 250. doi:10.3390/ijgi8060250 , 2019.

[8] Australian National Committee on Large Dams, "Guidelines on the consequence categories for dams.," Hobart, Tasmania: ANCOLD. , 2012.
[9] Federal Emergency Management Agency, , "Federal guidelines for inundation mapping of flood risks associated with dam incidents and failures (FEMA P-946)," Washington, DC: FEMA, US Department of Homeland Security. Available from: https://www.fema.gov/sites/ default/files/2020-08/fema_dam-safety_inundation-mapping-flood- risks.pdf [Accessed 28 Oct 2022], 2013.
[10] New Zealand Society on Large Dams, , "New Zealand dam safety guidelines. Wellington, New Zealand: NZSOLD. Available from:," https://nzsold.org.nz/wp-content/uploads/2019/10/nzsold_dam_ safety_guidelines-may-2015-1.pdf [Accessed 28 Oct 2022]. , 2015.
[11] Indian Central Water Commission, , "Guidelines for mapping flood risks associated with dams (CDSO_GUD_DS_05_v1.0). New Delhi, India," Central Water Commission, Central Dam Safety Organisation. Available from: https://damsafety.cwc.gov.in/ecm-includes/PDFs/ Guidelines_for_Mapping_Flood_Risks_Associated_with_Dams.pdf [Accessed 9 Nov 2022]. , 2018..
[12] Ashraf M, Soliman AH, El-Ghorab E, El Zawahry A, "Assessment of embankment dams breaching using large scale physical modeling and statistical methods.," Water Sci , vol. 32, no. 2 https:// doi. org/ 10. 1016/j. wsj. 2018. 05. 002 19. , p. 362–379. , 2018.
[13] Maddamsetty R, Praveen TV, Rao SS, Manjulavani K , "Tehri dam-breach versus monsoon flood routing in the ganga river system.," ISH J Hydraul Eng , vol. 16(1):, p. 109–131. https:// doi. org/ 10. 1080/ 09715 010. 2010. 10514 992 , 2010.
[14] Shwe PP, Kyaw S, " Modeling approach for earthen dam breach analysis in North Yamar Dam, Myanmar.," Technol Sci Am Sci Res J Eng , vol. 69(1):, p. 59–72 , 2020.
[15] Aureli F, Maranzoni A, Mignosa P, Ziveri C , "Dam-break flows: acquisition of experimental data through an imaging technique and 2D numerical modeling.," J Hydraul Eng):, vol. 134(8, no. https:// doi. org/ 10. 1061/ (asce) 0733, p. 1089–1101. , 2008.
[16] Leandro J, Martins R , "A methodology for linking 2D overland flow models with the sewer network model SWMM 5.1 based on dynamic link libraries.," Water Sci Technol , vol. 3017– 3026. https:// doi. org/ 10. 2166/ wst. 2016. 171 , p. 73(12):, 2016.
[17] Mujumdar PP, "Flood wave propagation.," Resonance, vol. 6(5):, no. https:// doi. org/ 10. 1007/ bf028 39085 , p. 66–73. , 2001.
[18] Frenette R, Munteanu A , "Vertically integrated numerical model to simulate breach formation by flow overtopping earth-filled dams: hydraulics.," J Hydraul Res , vol. 43(4):, no. https:// doi. org/ 10. 1080/ 00221 68050 95001 36, p. 408–416. , 2005.
[19] Shahrim MF, Ros FC , "Dam break analysis of temenggor dam using HEC-RAS," IOP Conf Ser Earth Environ Sci. , pp. https:// doi. org/ 10. 1088/ 1755- 1315/ 479/1/ 012041 , 2020.
[20] Rong G, Wang X, Xu H, Xiao B, "Multifactor regression analysis for predicting embankment dam breaching parameters.," J Hydraul Eng., no. https:// doi. org/ 10. 1061/ (asce) hy. 1943- 7900. 00016 53 , 2020.
[21] Foster M, Fell R, Spannagle M, "The statistics of embankment dam failures and accidents.," Can Geotech J 37(5):1000– 1024. https:// doi. org/ 10. 1139/ t00- 030 32. More Than 5,000 Dead in Libya as Collapsed Dams Worsen Flood Disaster - The New York Times. The statistics of embankment dam failures and accidents. Can Geotech J, pp. 37(5):1000–1024. https:// doi. org/ 10. 1139/ t00- 030, 2000.
[22] Froehlich DC , "Embankment dam breach parameters and their uncertainties.," Environ Prot , vol. 134:, p. 1708–1721 , 2008.
[23] Elfalan D , "Hawaii dam break analysis follow-on actions," World Environ Water Resour Congr , vol. https:// doi. org/ 10. 1061/ 40976 (316) 283 , p. 316:1–8. , 2008.
[24] Smemoe, C.M., et al., , "Demonstrating floodplain uncertainty using flood probability maps.," Journal of the American Water Resources Association, , Vols. 43 (2), doi:10.1111/j.1752-1688.2007.00028.x, p. 359–371., 2007.
[25] Vorogushyn, S., et al., , "A new methodology for flood hazard assessment considering dike breaches.," Water Resources Research,, Vols. 46 (8), . doi:10.1029/2009WR008475 , p. W08541, 2010.
[26] Tamiru H, Dinka MO, "Application of ANN and HEC-RAS model for flood inundation mapping in lower Baro Akobo River Basin. Ethiop," J Hydrol , vol. https:// doi. org/ 10. 1016/j. ejrh. 2021. 100855 , p. Reg Stud 36:100855. , 2021.
[27] Namara WG, Damisse TA, Tufa FG , "Application of HEC-RAS and HEC-GeoRAS model for flood inundation mapping, the case of Awash Bello Flood Plain, Upper Awash River Basin, Oromiya Regional State, Ethiopia.," Model Earth Syst Environ , vol. 8:, no. https:// doi. org/ 10. 1007/ s40808- 021- 01166-9 , p. 1449–1460. , 2022.
[28] Shahrim MF, Ros FC, "Dam break analysis of temenggor dam using hec-ras.," in IOP Conf Ser Earth Environ Sci 479(1):012041. https:// doi. org/ 10. 1088/ 1755- 1315/ 479/1/ 012041 , (2020).
[29] Cook AC , "Comparison of one-dimensional HEC-RAS with two-dimensional FESWMS model in flood inundation mapping.," in A thesis submitted to the Faculty of Purdue University, West Lafayette, Indiana , 2008.
[30] Brunner G, "Using HEC-RAS for Dam Breach Studies USACE HEC Technical," (2014) .
[31] Brunner G, "Using HEC-RAS for Dam Breach Studies, USACE HEC Technical," (2016) .

BIOGRAPHIES (Optional not mandatory)

Neman Sharif M M
Research Scholar,
Department of Civil Engineering,
University of Visvesvaraya College of Engineering,
Bangalore University, Bengaluru
nemansharifmm@gmail.com

Dr. Inayathulla M
Professor,
Department of Civil Engineering,
University of Visvesvaraya College of Engineering,
Bangalore University, Bengaluru
drinayath@gmail.com